Progress In Electromagnetics Research, Vol. 174, 23–32, 2022

Squeezing of Hyperbolic Polaritonic Rays in Cylindrical Lamellar Structures

Lu Song[1, 2], Lian Shen[2, 3, *], and Huaping Wang[1, *]

Abstract—We propose the squeezing of hyperbolic polaritonic rays in cylindrical lamellar structures with hyperbolic dispersion. This efficient design is presented through conformal mapping transformation by combining with circular effective-medium theory (CEMT) that is adopted to predict the optical response of concentric cylindrical binary metal-dielectric layers. The volume-confined hyperbolic polaritons supported in these cylindrical lamellar structures could be strongly squeezed when they propagate toward the origin since their wavelength shortens, and velocity decreases. To demonstrate the importance of using CEMT for engineering highly-squeezed hyperbolic polaritons, both CEMT and planar effective-medium theory (PEMT) are utilized to design the cylindrical lamellar structures. It is shown that the PEMT-based design is unable to achieve hyperbolic polaritons squeezing even with a sufficiently large number of metal-dielectric binary layers. Remarkably, this study opens new opportunities for the hyperbolic polaritons squeezing, and the findings are promising for propelling nanophotonics technologies and research endeavours.

1. INTRODUCTION

Light squeezing is recognized as a scientifically well-investigated method for generating intense subwavelength confined optical fields. The resultant strong field enhancement has opened up various potential applications, such as photodetection [1], singlephoton sources [2, 3], and nonlinear optics [4–6] through engineered antennas [7–9] and waveguides [10, 11], as well as the deep-subwavelength nanolithography in the industrially viable development [12, 13]. With the in-depth study of volume-confined hyperbolic polaritons [14–23] and the rapid advances in nanofabrication techniques, the squeezing of hyperbolic polaritons has recently attracted renewed attentions. Particularly, scientists show increased interests in utilizing hyperlens techniques for optical lithography [24–29]. The cylindrical lamellar structures with opposite signs of dielectric constants in the radial and tangential directions can support propagating waves with arbitrarily high wavenumbers [29] in principle. In this regard, it could be considered as a promising design for squeezing hyperbolic polaritons into the smallest possible or even point-like space.

The recently proposed transformation optics [30, 31] is a systemic-overall approach to constructing photonic devices not only on the macroscopic but also on the subwavelength scale, over the entire optical spectrum. This approach has already become the tool for building nanofocusing devices [28], invisibility cloaks [32–38], as well as singular plasmonic structures for light harvesting [39–41]. However, it is not obvious whether this approach could be successfully applied to the realm of highly-squeezed hyperbolic polaritons and further utilized to understand the effective-medium theory in cylindrical coordinates.

Received 21 March 2022, Accepted 26 April 2022, Scheduled 29 April 2022

* Corresponding author: Lian Shen (lianshen@zju.edu.cn), Huaping Wang (hpwang@zju.edu.cn).

[1] Key Laboratory of Ocean Observation-Imaging Testbed of Zhejiang Province, The Institute of Marine Electronics Engineering, Ocean College, Zhejiang University, Hangzhou 310027, China. [2] ZJU-Hangzhou Global Science and Technology Innovation Center, Key Lab. of Advanced Micro/Nano Electronic Devices & Smart Systems of Zhejiang, Zhejiang University, Hangzhou 310027, China. [3] Interdisciplinary Center for Quantum Information, State Key Laboratory of Modern Optical Instrumentation, College of Information Science and Electronic Engineering, Zhejiang University, Hangzhou 310027, China.

In this study, the squeezing of hyperbolic polaritonic rays is studied in a cylindrical lamellar structure with hyperbolic dispersion, which can be made of bilayers-thin alternating cylindrical layers of metal and dielectric. We theoretically propose that this cylindrical lamellar structure with hyperbolic dispersion could be analyzed via conformal mapping transformation and circular effective-medium theory (CEMT), which is able to squeeze the hyperbolic polaritons into a point-like space and enable broadband response. To showcase the importance of CEMT-based design for the hyperbolic polaritons, both CEMT and planar effective-medium theory (PEMT) are adopted to design the cylindrical hyperbolic metamaterials with the same materials and order of elemental layers. These two designs show totally different squeezing performances even with ultrathin elemental layers. The proposed analysis and design techniques could mitigate the technical and furthermore, may be utilized to design nanophotonic structures for photodetection, single-photon sources and other quantum emitters.

2. FUNDAMENTAL PRINCIPLE

2.1. Highly-Squeezed Hyperbolic Polaritons via a Conformal Mapping Transformation

We start with the analysis of how to squeeze hyperbolic polaritonic rays via a conformal mapping transformation. Consider an ideal situation: a transverse magnetic (TM) polarized emitter is located in near-field proximity to the interface of a planar lamellar structure with hyperbolic dispersion (see Figure 1(a)). In practice, the emission will efficiently couple to the hyperbolic polaritons (Poynting vector) and propagate toward the other interface with a propagation angle θ as shown in Figure 1(a), which is expressed as $\theta = \pm(\pi/2 - \varphi_c)$, where φ_c is the critical angle between the optical axis and the asymptotic line of hyperbolic iso frequency contours and satisfies the condition $\mathrm{Re}\left[\varepsilon(\varphi_c)\right] = 0$, in which

$$\varepsilon(\varphi)^{-1} = \cos^2(\varphi)(\varepsilon_\perp)^{-1} + \sin^2(\varphi)(\varepsilon_\parallel)^{-1}, \tag{1}$$

here φ is the angle between the wave vector of hyperbolic polaritons and the optical axis, and $\varepsilon_\perp$ and $\varepsilon_\parallel$ are the components perpendicular and parallel to the optical axis for the planar lamellar structure with hyperbolic dispersion, respectively. We then apply a known conformal mapping transformation, $\bar{z} = \bar{x} + i\bar{y} \rightarrow \bar{w} = \bar{u} + i\bar{v}$, as shown in Figure 1,

$$\bar{z} = \bar{\rho}e^{(i\bar{\phi})} = \rho_{l_{\max}} e^{\bar{w}/\kappa} = \left(\rho_{l_{\max}} e^{\bar{u}/\kappa}\right)\left(e^{i\bar{v}/\kappa}\right), \tag{2}$$

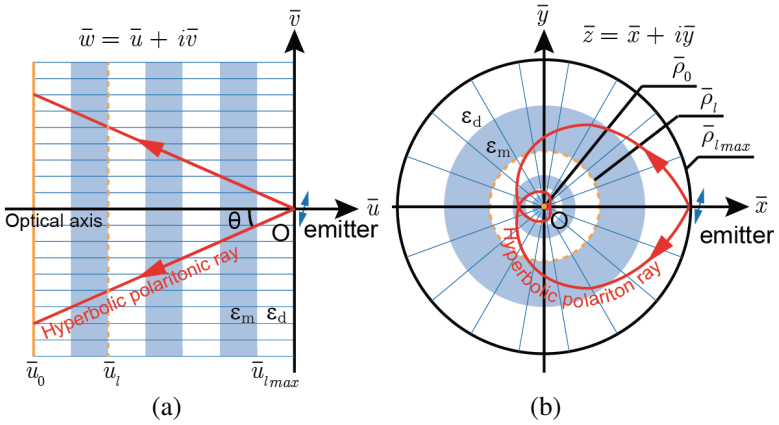

Figure 1. Fundamental principle of the highly-squeezed hyperbolic polaritons via a conformal mapping transformation. It maps the planar lamellar layers onto the concentric layers of cylindrical structure with a known conformal mapping transformation $\bar{z} = \bar{x} + i\bar{y} \rightarrow \bar{w} = \bar{u} + i\bar{v}$. (a) A slab (semi-infinite or finite) of a planar lamellar structure with hyperbolic dispersion supports volume-confined hyperbolic polaritons which could transport its energy to the end. The spectrum is continuous and broadband therefore the process is efficient over a wide range of wavelengths. (b) The transformed space of (a) is an ordered cylindrical lamellar structure with hyperbolic dispersion.

where $\bar{u}$ and $\bar{v}$ are the real space coordinates, while $\bar{\rho}$ and $\bar{\phi}$ are their transformed counterparts; κ is the scaled factor for the two structures; $\bar{u}_{l_{\max}} = 0$ is mapped into the radius $\bar{\rho}_{l_{\max}}$, which is selected arbitrarily. Thus, the coordinates are connected by,

$$\bar{\rho} = \rho_{l_{\max}} e^{\bar{u}/\kappa}, \quad \bar{\phi} = \bar{v}/\kappa. \tag{3}$$

If the slab is semi-infinite $\bar{u}_0 \to -\infty$, which means that the orange line in $\bar{w}$ translates to the origin in $\bar{z}$ and the dark line in $\bar{w}$ translates to the external circle in $\bar{z}$ as shown in Figure 1. Transformation optics enables us to obtain the physical insight into this process. A polarized emitter generates hyperbolic polaritons in the planar hyperbolic media which could transport to infinity without reflection. The spectrum of hyperbolic polaritons is continuous in the wavelength range with hyperbolic dispersion. Upon the transformation, infinity is mapped to the origin. Hence, in the transformed frame, hyperbolic polaritons are squeezed to the origin without reflection. In practice, material losses and finite thicknesses of the discrete constituent elements used in the realization of the hyperbolic metamaterials may relax the degree of confinement of hyperbolic polaritons, thereby broadening the angular distribution of the emission and limiting the propagation length of hyperbolic polaritons. In this regard, the word "infinity" means the limited propagation length of hyperbolic polaritons, thus the hyperbolic polaritons in the transformed space will not be rigorously squeezed at the origin but into a small region. To understand the hyperbolic polaritons squeezing in this case, we could still follow the conformal mapping transformation mentioned in Figure 1, that is if the slab is extremely large but finite, the orange line in $\bar{w}$ translates to a small circle in $\bar{z}$ while the dark line in $\bar{w}$ translates to the external circle in $\bar{z}$. Thus, the hyperbolic polaritons will be squeezed at the edge of the small inner circle.

Now we move to the determination of material parameters in the transformed space. We introduce a two-dimensional Jacobian matrix $J = \begin{pmatrix} \partial x/\partial u & \partial x/\partial v \\ \partial y/\partial u & \partial y/\partial v \end{pmatrix}$, thus the permittivity and permeability tensors in transformed space become,

$$\varepsilon' = \mathrm{diag}\left(\varepsilon_\perp \varepsilon_\parallel\right), \quad \mu' = \mu_0 \det(J)^{-1}. \tag{4}$$

We notice that the design of hyperbolic polaritons squeezing based on cylindrical lamellar structure involves spatial dependent permeability along the out-of-plane direction, which is difficult to implement in visible and infrared spectrum. To excite hyperbolic polaritons, we could consider the electrostatic approximation model: a system in which all dimensions are smaller than the wavelength of light. We assume that the radiative effects decoupling electrostatic and magnetostatic fields can be neglected to ease the discussion. As a consequence, we can ignore the contribution from permeability and assume that it is equal to unity, thus Eq. (4) can be simplified as,

$$\varepsilon' = \mathrm{diag}\left(\varepsilon_\phi \varepsilon_\rho\right) \mu' = 1. \tag{5}$$

where ε_ϕ and ε_ρ are the components in the directions of $\bar{\phi}$ and $\bar{\rho}$, respectively.

2.2. Bloch Theorem and Effective-Medium Theory

To realize hyperbolic polaritons squeezing in quasistatic limit, an approximation technique is needed, where the cylindrical hyperbolic metamaterial can be constructed by a number of alternative metal and dielectric layers, as shown in Figure 1(b). Since the effective permittivity tensors for planar and cylindrical hyperbolic lamellar structures are the same, the effective material properties of a planar lamellar structure (see Figure 1(a)) with period Λ ($\Lambda = u_{l+2} - u_l$) will be first studied, which can be obtained from the following equation according to the Bloch theorem [42],

$$\begin{aligned} \cos\left(K\Lambda\right) \;=\; & \cos\left[k_1\left(u_{l+1} - u_l\right)\right]\cos\left[k_2\left(u_{l+2} - u_{l+1}\right)\right] \\ & -\gamma \sin\left[k_1\left(u_{l+1} - u_l\right)\right]\sin\left[k_2\left(u_{l+2} - u_{l+1}\right)\right], \end{aligned} \tag{6}$$

where $\gamma_{\mathrm{TM}} = 1/2\left(\varepsilon_m k_1/\varepsilon_d k_2 + \varepsilon_d k_2/\varepsilon_m k_1\right)$ is for the TM-polarized waves, $\gamma_{\mathrm{TE}} = 1/2\left(\varepsilon_m/\varepsilon_d + \varepsilon_d/\varepsilon_m\right)$ is for the transverse electric (TE) polarized waves and $k_{1,2}^2 = \varepsilon_{d,m} k_0^2 - \beta^2$, β represents the component of wave vector in the direction of $\bar{v}$. Hence, a series expansion of Eq. (6) yields a conventional zeroth-order PEMT,

$$\varepsilon_{u,l}^{-1}\left(u_{l+2} - u_l\right) \;=\; \varepsilon_l^{-1}\left(u_{l+1} - u_l\right) + \varepsilon_{l+1}^{-1}\left(u_{l+2} - u_{l+1}\right) \tag{7}$$

$$\varepsilon_{v,l}\left(u_{l+2} - u_l\right) \;=\; \varepsilon_l\left(u_{l+1} - u_l\right) + \varepsilon_{l+1}\left(u_{l+2} - u_{l+1}\right) \tag{8}$$

where $\varepsilon_l = \varepsilon_{l+2} = \varepsilon_d$ and $\varepsilon_{l+1} = \varepsilon_{l+3} = \varepsilon_m$, thus hyperbolic dispersion can be achieved by arranging periodic subwavelength thin layers of metal and dielectric homogeneous materials carefully.

Under the transformation, $\bar{z} = \bar{x} + i\bar{y} \rightarrow \bar{w} = \bar{u} + i\bar{v}$, the effective material properties remain unchanged; however, the dimensions change according to Eq. (3). To obtain the effective-medium theory and accomplish hyperbolic dispersion in this transformed space with the same materials and order of elemental layers, we turn to study how the Bloch theorem is modified. If a material has periodicity such as $n(u) = n(u+\Lambda)$, as it is the case in planar layered structure as shown in Figure 1(a), wave propagation in such a medium is represented by

$$F_K(u) = F(u)\exp(-iKu), \tag{9}$$

according to the Floquet theorem [42, 43]. Here, K indicates the Bloch wavenumber common in the periodic structure, and $F_K(u)$ is the periodic function with period $\Lambda = u_{l+2} - u_l$, namely,

$$F_K(u+\Lambda) = F_K(u) \rightarrow F(u+\Lambda) = \exp(-iK\Lambda)F(u). \tag{10}$$

Since the quantity $\bar{k}\cdot\bar{r}$ must remain unchanged under the transformation, the wave vector in the transformed frame can be calculated as,

$$\bar{k}' = \left(J^T\right)^{-1}\bar{k}. \tag{11}$$

Here, superscripts prime refers to parameters in the transformation space. Thus, we could come to the same conclusion for the Bloch wavenumber,

$$\bar{K}' = \left(J^T\right)^{-1}\bar{K}. \tag{12}$$

In this situation, the wave propagation according to the Floquet theorem in the transformed space is represented by,

$$\mathcal{F}_{K'}(\rho) = \mathcal{F}(\rho)\exp\left(-iK'\rho\right), \tag{13}$$

where K' indicates the Bloch wavenumber common in the transformed space, and $\mathcal{F}_{K'}(\rho)$ is the periodic function with period Λ', thus

$$\mathcal{F}_{K'}\left(\rho+\Lambda'\right) = \mathcal{F}_{K'}(\rho) \rightarrow \mathcal{F}\left(\rho+\Lambda'\right) = \exp\left(-iK'\Lambda'\right)\mathcal{F}(\rho). \tag{14}$$

Therefore, in the quasistatic approximation model, according to the conformal mapping in Eq. (3), we could obtain the following eigenvalue equation in cylindrical hyperbolic metamaterial which can be constructed by a number of alternative metal and dielectric layers

$$\begin{aligned}\cos\left(K'\Lambda'\right) \;=\; & \cos\left[k_1'\kappa\ln\left(\rho_{l+1}/\rho_l\right)\right]\cos\left[k_2'\kappa\ln\left(\rho_{l+2}/\rho_{l+1}\right)\right] \\ & -\gamma'\sin\left[k_1'\kappa\ln\left(\rho_{l+1}/\rho_l\right)\right]\sin\left[k_2'\kappa\ln\left(\rho_{l+2}/\rho_{l+1}\right)\right]\end{aligned} \tag{15}$$

and further the zeroth-order CEMT,

$$\varepsilon_{\rho,l}^{-1}\ln\left(\rho_{l+2}/\rho_l\right) \;=\; \varepsilon_l^{-1}\ln\left(\rho_{l+1}/\rho_l\right) + \varepsilon_{l+1}^{-1}\ln\left(\rho_{l+2}/\rho_{l+1}\right), \tag{16}$$

$$\varepsilon_{\phi,l}\ln\left(\rho_{l+2}/\rho_l\right) \;=\; \varepsilon_l\ln\left(\rho_{l+1}/\rho_l\right) + \varepsilon_{l+1}\ln\left(\rho_{l+2}/\rho_{l+1}\right) \tag{17}$$

Previously, an improved effective-medium approximation has been applied to obtain nonlocal corrections for anisotropic materials made of lamellar structures with subwavelength thin layers [44]. According to the above discussion, a parallel work about the nonlocal adjustments for the cylindrical systems can be straightforwardly calculated in a way much similar to the techniques introduced here.

For CEMT-based design, as demonstrated in Eq. (3), we have the following relation

$$\rho_{l+1} = \rho_l\exp\left[\left(u_{l+1}-u_l\right)/\kappa\right] \rightarrow \rho_{l_{\max}} = \rho_0\prod_0^{l_{\max}}\exp\left[\left(u_{l+1}-u_l\right)/\kappa\right] \tag{18}$$

where $\kappa = l_{\max}\left(u_{l+2}-u_l\right)/\left[2\ln\left(\rho_{l_{\max}}/\rho_0\right)\right]$ is defined to fit both inner and outer radii. Therefore, for a given number of layers $l_{\max}$, the inner radius ρ_0 and outer radius $\rho_{l_{\max}}$, the entire design can be achieved.

3. RESULTS AND DISCUSSIONS

As discussed previously, the lamellar structures with hyperbolic dispersion (see Figure 1) can be achieved by arranging periodic subwavelength thin layers of metal and dielectric homogeneous materials. As an example, we consider silver as the metal layers, and for its permittivity, we use the Drude model,

$$\varepsilon_m = \varepsilon_\infty - \omega_p^2 / \left[\omega\left(\omega + i\omega_c\right)\right], \tag{19}$$

with $\varepsilon_\infty = 3.8355$, $\omega_p = 1.3937 \times 10^{16}$ rad/s and $\omega_c = 2.9588 \times 10^{13}$ rad/s [45]. The dielectric layer is silica with a permittivity of $\varepsilon_d = 2.25$.

In order to achieve the squeezing of hyperbolic polaritons in cylindrical lamellar structure, the effective permittivity tensor for planar lamellar structure should be first considered as depicted in Figure 2(a) according to Eqs. (7) and (8). For simplicity, same-sized metal and dielectric layers are chosen here ($u_{l+2} - u_{l+1} = u_{l+1} - u_l$). From this figure, we find that this planar lamellar structure clearly exhibits hyperbolic properties in the wavelength range 500 nm–2500 nm. According to Eq. (5), we could reveal that the corresponding components of the effective permittivity tensor for both planar and cylindrical hyperbolic lamellar structures are the same, thus we show ε_ϕ and ε_ρ in the figure directly instead of $\varepsilon_\perp$ and $\varepsilon_\parallel$. Due to the dispersion of hyperbolic metamaterial, the propagation angle of the hyperbolic polaritons according to Eq. (1) is sensitive to the wavelength as shown at the bottom of Figure 2(a).

In the literature, cylindrical hyperbolic metamaterials for subwavelength imaging and focusing have already been investigated, but the case of a cylindrical hyperbolic metamaterial for squeezing hyperbolic polaritons into a point-like space has never been addressed to the best of our knowledge. As we will see, the cylindrical lamellar structure operates efficiently over a broadband range from visible to mid-infrared

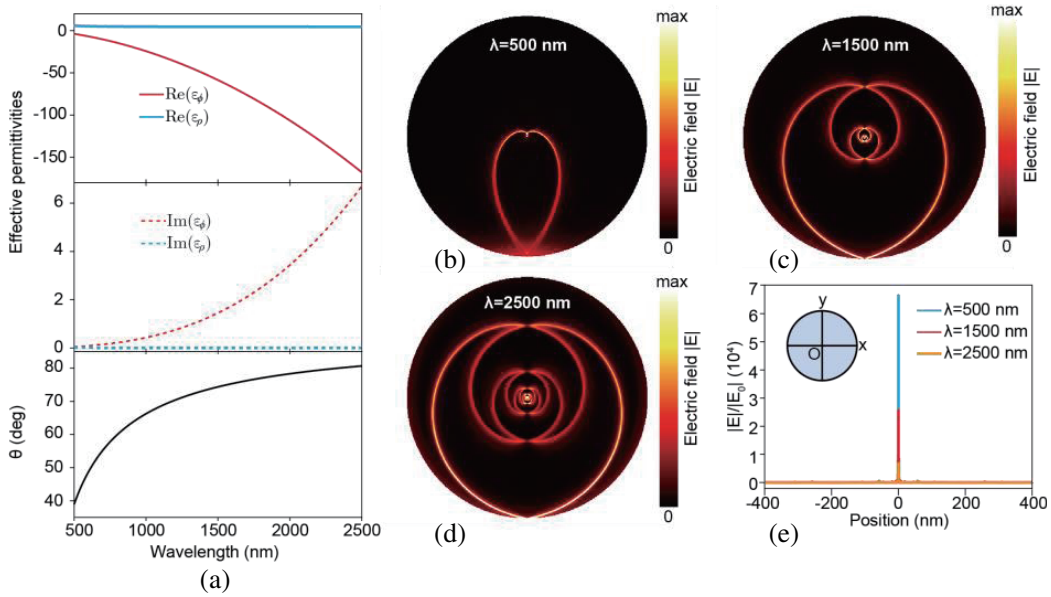

Figure 2. Highly-squeezed hyperbolic polaritons with effective model. (a) Optical properties of the hyperbolic lamellar structure with alternating silver and silica layers. The components of the effective permittivity tensor and the propagation angle as a function of wavelength [top, Re(ε_ϕ) and Re(ε_ρ); middle Im(ε_ϕ) and Im(ε_ρ); bottom, θ] are shown. Wavelengths of 500 nm–2500 nm are considered since the lamellar structure in this range has hyperbolic dispersion. (b)–(d) Simulated electric-field magnitudes at different wavelengths: (b) 500 nm, (c) 1500 nm, (d) 2500 nm generated by the TM polarized emitter. In these simulations, a 400 nm radius cylindrical structure with hyperbolic dispersion is used to realize highly-squeezed hyperbolic polaritons. (e) The amplitude of the electric field along a cross-section close to the origin of the cylindrical structure. The electric-field enhancement is normalized with respect to the electric-field magnitude in free space.

spectrum since hyperbolic properties can be achieved in this spectrum. According to Eqs. (11) and (12), the wave vector of the hyperbolic polaritons becomes infinite as they approach the origin. Therefore, hyperbolic polaritons propagate toward the origin as their wavelength shortens, and velocity decreases. This fact is ensured by the theory of transformation optics, that is if we transform infinity to a finite point, the velocity automatically taken by the transformation must be zero at this point. Besides, the cylindrical hyperbolic metamaterial has a singularity in the material parameters at the origin. This material singularity has the same function as the geometrical singularity of previous studies [39–41], and hence will stop hyperbolic polaritons approaching the origin. In an ideal lossless hyperbolic metamaterial, energy accumulates toward the origin, its density increasing with time without bound. In practice, material losses will resolve the situation leading to a balance between energy accumulation and dissipation.

To demonstrate the squeezing performance of hyperbolic polaritons according to conformal mapping transformation, we first conduct field mapping simulations using a commercial finite-element method based solver (COMSOL MULTIPHYSICS). Simulated electric-field magnitudes of the squeezed hyperbolic polaritons at different wavelengths (500 nm, 1500 nm, and 2500 nm) for effective model are depicted in Figures 2(b)–(e). In these simulations, a TM polarized emitter is located near a 400 nm radius cylindrical structure with hyperbolic dispersion. From Figures 2(b)–(d), we find that hyperbolic polaritionic rays spiral gradually towards the origin from the emitter. To gain more insight into the behavior of the fields around the origin, the line profiles of electric-field enhancement along a cross-section close to the origin are also shown in Figure 2(e) for different wavelengths. The electric-field enhancement here is normalized with respect to the electric-field magnitude in free space. From the plot, it is observed that near the origin, a clear electric-field enhancement is observed as the hyperbolic polaritons become more strongly concentrated. The result of the electric-field enhancement on increasing the wavelength is also shown in the plot in Figure 2(e), in which $\mathrm{Im}(\varepsilon_\phi)$ increases when the wavelength is increased, which greatly reduces the electric-field enhancement. One thing to note is that the squeezing of hyperbolic polaritons can be realized at different wavelengths, although losses as the function of wavelength truncate the growth of the field at the origin.

After we obtain the phenomena of hyperbolic polaritons squeezing for the effective model, the next question that arises is what happens to the practical implementation of the proposed hyperbolic polaritons squeezing device. As mentioned above, the effective model of cylindrical lamellar structure has a singularity in the material parameters at the origin. However, to avoid this singularity while still maintaining hyperbolic polaritons squeezing, the inner radius should be small enough compared to the wavelength. The physical insight for this case has been explained above, thus in a practical cylindrical lamellar structure we expect that the hyperbolic polaritons will be squeezed at the edge of the inner circle. Usually, the PEMT based on Eqs. (7) and (8) is applied to design the optical properties of cylindrical lamellar structure; however, this is not always valid especially for hyperbolic polaritons. To further investigate this, both CEMT and PEMT are adopted to the design of cylindrical lamellar structure. In these simulations, the squeezing device with the sufficient number of layers $l_{\max} = 100$, the inner radius $\rho_0 = 10\,\mathrm{nm}$, and the outer radius $\rho_{l_{\max}} = 400\,\mathrm{nm}$ is demonstrated. The thickness of each layer for CEMT-based design can be obtained via Eq. (18).

Figure 3 shows the results of PEMT- and CEMT-based designs for cylindrical lamellar structures. Simulated electric-field magnitudes of the squeezed hyperbolic polaritons at different wavelengths (500 nm, 1500 nm, and 2500 nm) for PEMT- and CEMT-based designs are shown in Figures 3(a)–(f). From these figures, we could find that for PEMT-based design, the hyperbolic polaritons could not be squeezed when they propagate into the origin. Nevertheless, for CEMT-based design, most of the hyperbolic polaritons could spiral gradually towards the origin and squeeze at the edge of the inner circle. From the line profiles of electric-field enhancement shown in Figures 3(g)–(i), it could be clearly observed that the CEMT-based design continues to perform well and could squeeze hyperbolic polaritons into a point-like space at the edge of the inner circle, although the back reflection at the interface of each layer decreases the electric-field enhancement. However, for the PEMT-based design, the peak of electric-field enhancement vanishes and no hyperbolic polaritons squeeze at the edge of the inner circle. This is because the wave vector of the hyperbolic polaritons increases as they approach the origin, and Eq. (12) for Bloch wavenumber is not satisfied. At this point, the cylindrical lamellar structure based on PEMT can no longer be treated as an effective medium, and the hyperbolic polaritons are cut off,

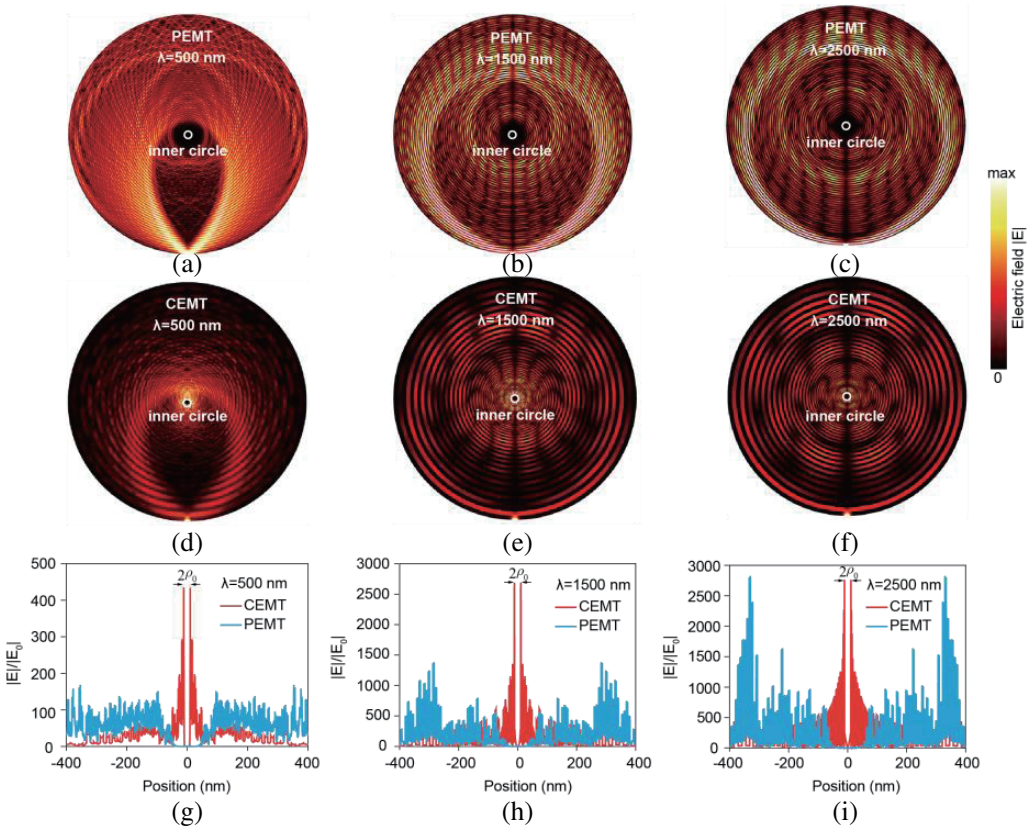

Figure 3. Highly-squeezed hyperbolic polaritons with discrete pairs of binary metal-dielectric layers. Both PEMT and CEMT are adopted to the design of cylindrical lamellar structure. (a)–(f) Simulated electric-field magnitudes of the squeezed hyperbolic polaritons at different wavelengths: (a), (d) 500 nm, (b), (e) 1500 nm, (c), (f) 2500 nm generated by the TM polarized emitter, (g), (h), (i) the amplitude of the electric field along a cross section close to the origin of the cylindrical lamellar structure. The electric-field enhancement is normalized with respect to the electric-field magnitude in free space.

leading to the invalidation of the squeezing device. We could conclude that in this case there is a substantial performance gap between the PEMT- and CEMT-based designs. In addition, the squeezing is strongly related to the wavelength; however for a longer wavelength (2500 nm), the loss increases, which reduces the electric-field enhancement (Figure 3(i)). Anyhow, the CEMT-based design could still squeeze the hyperbolic polaritons into a point-like space at the edge of the inner circle, although more energy is dissipated.

In a nutshell, all our simulation cases including the effective model and discrete pairs of binary metal-dielectric layers showcase a good squeezing performance achieved through the conformal mapping based CEMT design. The proposed design procedure is general and can be utilized as an innovatory way to robust hyperbolic polaritons squeezing.

4. CONCLUSIONS

To summarize, using the formalism of conformal mapping transformation optics, we extend the concept of hyperbolic polaritons squeezing and demonstrate how the hyperbolic polaritons propagate toward the singularity where the velocity vanishes. Strong electric-field enhancement ($\sim 10^4$) and confinement are predicted within the classical approach. We also show that the proposed effective model can be substituted by a cylindrical lamellar structure using two distinct designs PEMT and CEMT. Numerical simulations of the effective model and the lamellar devices illuminated with a TM polarized emitter indicate that the CEMT-based design demonstrates superior squeezing performance versus the PEMT-

based design with the same materials and order of elemental layers. In fact, the conventional PEMT fails to adequately approximate the optical properties of the cylindrical lamellar structure for squeezing of hyperbolic polaritonic rays even with a sufficiently large number of metal-dielectric binary layers which is different from our previous work for nanofocusing [28]. From the conformal mapping point of view, we identify the quantity $\bar{k} \cdot \bar{r}$ to be the cause of this disagreement. The wave vector $\bar{k}$ becomes extremely large if hyperbolic polaritons are squeezed into a smallest possible or even point-like space, $\bar{r} \to 0$. Although PEMT-based design is much easier for constructing an arbitrary lamellar structure, conformal mapping based CEMT is necessary for the design of hyperbolic polaritons squeezing device. Moreover, we highlight that due to the advancement of nanotechnology, it might be feasible to implement cylindrical lamellar structures in experiments [46, 47]. Because of its ease of applicability, we anticipate that this approach based on hyperbolic polaritons will find great potential applications in solar cells, spectroscopy, medical applications, and quantum information.

ACKNOWLEDGMENT

National Natural Science Foundation of China (61905216, 61775193).

REFERENCES

1. Tang, L., S. E. Kocabas, S. Latif, A. K. Okyay, D.-S. Ly-Gagnon, K. C. Saraswat, and D. A. B. Miller, "Nanometre-scale germanium photodetector enhanced by a near-infrared dipole antenna," *Nat. Photonics*, Vol. 2, No. 4, 226, 2008.
2. Yuan, Z., B. E. Kardynal, R. M. Stevenson, A. J. Shields, C. J. Lobo, K. Cooper, N. S. Beattie, D. A. Ritchie, and M. Pepper, "Electrically driven single-photon source," *Science*, Vol. 295, 102, 2002.
3. Akimov, A. V., A. Mukherjee, C. L. Yu, D. E. Chang, A. S. Zibrov, P. R. Hemmer, H. Park, and M. D. Lukin, "Generation of single optical plasmons in metallic nanowires coupled to quantum dots," *Nature*, Vol. 450, 402, 2007.
4. Park, I. Y., S. Kim, J. Choi, D. H. Lee, Y. J. Kim, M. F. Kling, M. I. Stockman, and S. W. Kim, "Plasmonic generation of ultrashort extreme-ultraviolet light pulses," *Nat. Photonics*, Vol. 5, 677, 2011.
5. Sederber, S. and A. Y. Elezzabi, "Ponderomotive electron acceleration in a silicon-based nanoplasmonic waveguide," *Phys. Rev. Lett.*, Vol. 113, 167401, 2014.
6. Wang, K., H. Qian, Z. Liu, and P. K. L. Yu, "Second-order nonlinear susceptibility enhancement in gallium nitride nanowires," *Progress In Electromagnetics Research*, Vol. 168, 25–30, 2020.
7. Aouani, H., M. Rahmani, M. Navarro-Cía, and S. A. Maier, "Third-harmonic-upconversion enhancement from a single semiconductor nanoparticle coupled to a plasmonic antenna," *Nat. Nanotechnol.*, Vol. 9, 290, 2014.
8. Kim, S., J. Jin, Y. J. Kin, I. Y. Park, Y. Kim, and S. W. Kim, "High-harmonic generation by resonant plasmon field enhancement," *Nature*, Vol. 453, 757, 2008.
9. Beneck, R. J., A. Das, G. Mackertich-Sengerdy, R. J. Chaky, Y. Wu, S. Soltani, and D. Werner, "Reconfigurable antennas: A review of recent progress and future prospects for next generation," *Progress In Electromagnetics Research*, Vol. 171, 89–121, 2021.
10. Choo, H., M. K. Kim, M. Staffaroni, T. J. Seok, J. Bokor, S. Cabrini, P. J. Schuck, M. C. Wu, and E. Yablonovitch, "Nanofocusing in a metal-insulator-metal gap plasmon waveguide with a three-dimensional linear taper," *Nat. Photonics*, Vol. 6, 838–844, 2012.
11. Stockman, M. I., "Nanofocusing of optical energy in tapered plasmonic waveguides," *Phys. Rev. Lett.*, Vol. 93, 137404, 2004.
12. Srituravanich, W., L. Pan, Y. Wang, C. Sun, D. B. Bogy, and X. Zhang, "Flying plasmonic lens in the near field for high-speed nanolithography," *Nat. Nanotechnol.*, Vol. 3, 733, 2008.
13. Wagner, C. and N. Harned, "Lithography gets extreme," *Nat. Photonics*, Vol. 4, 24, 2010.

14. Sternbach, A. J., S. H. Chae, S. Latini, A. A. Rikhter, Y. Shao, B. Li, D. Rhodes, B. Kim, P. J. Schuck, X. Xu, X. Y. Zhu, R. D. Averitt, H. Hone, M. M. Fogler, A. Rubio, and D. N. Basov, "Programmable hyperbolic polaritons in van der Waals semiconductors," *Science*, Vol. 371, 5529, 2021.
15. Chen, M., X. Lin, T. H. Dinh, Z. Zheng, J. Shen, Q. Ma, H. Chen, P. Jarillo-Herrero, and S. Dai, "Configurable phonon polaritons in twisted α-MoO_3," *Nat. Mater.*, Vol. 19, 1307, 2020.
16. Sedov, E. S., I. V. Iorsh, S. M. Arakelian, A. P. Alodjants, and A. Kavokin, "Hyperbolic metamaterials with Bragg polaritons," *Phys. Rev. Lett.*, Vol. 114, 237402, 2015.
17. Yoxall, E., M. Schnell, A. Y. Nikitin, O. Txoperena, A. Woessner, M. B. Lundeberg, F. Casanova, L. E. Hueso, F. H. Koppens, and R. Hillenbrand, "Direct observation of ultraslow hyperbolic polariton propagation with negative phase velocity," *Nat. Photonics*, Vol. 9, 674, 2015.
18. Caldwell, J. D., A. V. Kretinin, Y. Chen, V. Giannini, M. M. Fogler, Y. Francescato, C. T. Ellis, J. G. Tischler, C. R. Woods, A. J. Giles, M. Hong, K. Watanabe, T. Taniguchi, S. A. Maier, and K. S. Novoselov, "Sub-diffractional volume-confined polaritons in the natural hyperbolic material hexagonal boron nitride," *Nat. Commun.*, Vol. 5, 5221, 2014.
19. Li, P., M. Lewin, A. V. Kretinin, J. D. Caldwell, K. S. Novoselov, T. Taniguchi, K. Watanabe, F. Gaussmann, and T. Taubner, "Hyperbolic phonon-polaritons in boron nitride for near-field optical imaging and focusing," *Nat. Commun.*, Vol. 6, 7507, 2015.
20. Dai, S., Q. Ma, T. Andersen, A. Mcleod, Z. Fei, M. Liu, M. Wagner, K. Watanabe, T. Taniguchi, M. Thiemens, F. Keilmann, P. Jarillo-Herrero, M. M. Fogler, and D. N. Basov, "Subdiffractional focusing and guiding of polaritonic rays in a natural hyperbolic material," *Nat. Commun.*, Vol. 6, 6963, 2015.
21. Alfaro-Mozaz, F. J., P. Alonso-González, S. Vélez, I. Dolado, M. Autore, S. Mastel, F. Casanova, L. E. Hueso, P. Li, A. Y. Nikitin, and R. Hillenbrand, "Nanoimaging of resonating hyperbolic polaritons in linear boron nitride antennas," *Nat. Commun.*, Vol. 8, 15624, 2017.
22. Shen, L., X. Lin, M. Shalaginov, T. Low, X. Zhang, B. Zhang, and H. Chen, "Broadband enhancement of on-chip single-photon extraction via tilted hyperbolic metamaterials," *Appl. Phys. Rev.*, Vol. 7, 021403, 2020.
23. Ishii, S., A. V. Kildishev, E. Narimanov, V. M. Shalaev, and V. P. Drachev, "Sub-wavelength interference pattern from volume plasmon polaritons in a hyperbolic medium," *Laser & Photon. Rev.*, Vol. 7, 265, 2013.
24. Liu, Z., H. Lee, Y. Xiong, C. Sun, and X. Zhang, "Far-field optical hyperlens magnifying sub-diffraction-limited objects," *Science*, Vol. 315, 5819, 1686, 2007.
25. Rho, J., Z. Ye, Y. Xiong, X. Yin, Z. Liu, H. Choi, G. Bartal, and X. Zhang, "Spherical hyperlens for two-dimensional sub-diffractional imaging at visible frequencies," *Nat. Commun.*, Vol. 1, 143, 2010.
26. Sun, J., M. I. Shalaev, and N. M. Litchinitser, "Experimental demonstration of a non-resonant hyperlens in the visible spectral range," *Nat. Commun.*, Vol. 6, 7201, 2015.
27. Xiong, Y., Z. Liu, and X. Zhang, "Projecting deep-subwavelength patterns from diffraction-limited masks using metal-dielectric multilayers," *Appl. Phys. Lett.*, Vol. 93, 111116, 2008.
28. Shen, L., A. V. Kildishev, and H. Chen, "Designing optimal nanofocusing with a gradient hyperlens," *Nanophotonics*, Vol. 7, 479, 2018.
29. Jacob, Z., L. V. Alekseyev, and E. Narimanov, "Optical hyperlens: Far-field imaging beyond the diffraction limit," *Opt. Express*, Vol. 14, 8247, 2006.
30. Pendry, J. B., D. Schurig, and D. R. Smith, "Controlling electromagnetic fields," *Science*, Vol. 312, 1780, 2006.
31. Leonhardt, U., "Optical conformal mapping," *Science*, Vol. 23, 1777, 2006.
32. Shen, L., B. Zheng, Z. Liu, Z. Wang, S. Lin, S. Dehdashti, E. Li, and H. Chen, "Large-scale far-infrared invisibility cloak hiding object from thermal detection," *Adv. Opt. Mater.*, Vol. 112, 7635, 2015.

33. Chen, H., B. Zheng, L. Shen, H. Wang, X. Zhang, N. Zheludev, and B. Zhang, "Ray-optics cloaking devices for large objects in incoherent natural light," *Nat. Commun.*, Vol. 4, 2652, 2013.
34. Chen, H., B. Wu, B. Zhang, and J. Kong, "Electromagnetic wave interactions with a metamaterial cloak," *Phys. Rev. Lett.*, Vol. 99, 063903, 2007.
35. Xi, S., H. Chen, B. Wu, and J. Kong, "One-directional perfect cloak created with homogeneous material," *IEEE Microw. Wireless Compon. Lett.*, Vol. 19, No. 3, 131, 2009.
36. Zhang, B., H. Chen, B. Wu, and J. Kong, "Extraordinary surface voltage effect in the invisibility cloak with an active device inside," *Phys. Rev. Lett.*, Vol. 100, 063904, 2008.
37. Qian, C., B. Zheng, Y. Shen, L. Jing, E. Li, L. Shen, and H. Chen, "Deep-learning-enabled self-adaptive microwave cloak without human intervention," *Nat. Photonics*, Vol. 14, 383, 2020.
38. Xu, S., X. Cheng, S. Xi, R. Zhang, H. Moser, Z. Shen, Y. Xu, Z. Huang, X. Zhang, F. Yu, B. Zhang, and H. Chen, "Experimental demonstration of a free space cylindrical cloak without superluminal propagation," *Phys. Rev. Lett.*, Vol. 109, 223903, 2012.
39. Aubry, A., D. Y. Lei, A. I. Fernández-Domínguez, Y. Sonnefraud, S. A. Maier, and J. B. Pendry, "Plasmonic light-harvesting devices over the whole visible spectrum," *Nano Lett.*, Vol. 10, 2574, 2010.
40. Pendry, J. B., A. I. Fernández-Domínguez, Y. Luo, and R. Zhao, "Capturing photons with transformation optics," *Nat. Phys.*, Vol. 9, 518, 2013.
41. Luo, Y., D. Y. Lei, S. A. Maier, and J. B. Pendry, "Broadband light harvesting nanostructures robust to edge bluntness," *Phys. Rev. Lett.*, Vol. 108, 023901, 2012.
42. Yeh, P., A. Yariv, and E. Marom, "Electromagnetic propagation in periodic stratified media. I. General theory," *J. Opt. Soc. Am.*, Vol. 67, 423, 1977.
43. Yeh, P., *Optical Waves in Layered Media*, Wiley, New York, 1988.
44. Elser, J. and V. A. Podolskiy, "Nonlocal effects in effective-medium response of nanolayered metamaterials," *Appl. Phys. Lett.*, Vol. 90, 191109, 2007.
45. Johnson, P. B. and R. W. Christy, "Optical constants of the noble metals," *Phys. Rev. B*, Vol. 6, No. 12, 4370, 1972.
46. Johnson, R. W., A. Hultqvist, and S. F. Bent, "A brief review of atomic layer deposition: From fundamentals to applications," *Mater. Today*, Vol. 17. 236–246, 2016.
47. Bassim, N., K. Scott, and L. A. Giannuzzi, "Recent advances in focused ion beam technology and applications," *MRS Bulletin*, Vol. 39, 317–325, 2014.